

MiR-30a-5p ameliorates LPS-induced inflammatory injury in human A549 cells and mice via targeting RUNX2

Innate Immunity
2021, Vol. 27(1) 41–49
© The Author(s) 2020
Article reuse guidelines:
sagepub.com/journals-permissions
DOI: 10.1177/1753425920971347
journals.sagepub.com/home/ini
SAGE

Pibao Li^{1,2}, Yanfen Yao², Yuezhen Ma² and Yanbin Chen¹ 

Abstract

In this study, we aim to investigate the role of miR-30a-5p in acute lung injury/acute respiratory distress syndrome (ALI/ARDS) using LPS-induced A549 cells and mice. We found cell viability was significantly declined accompanied by cell apoptosis and cell cycle arrest at G0/G1 phase in LPS-treated A549 cells. MiR-30a-5p was down-regulated by LPS treatment and miR-30a-5p significantly protected A549 cells from LPS-induced injury by increasing cell viability, reducing cell apoptosis, promoting cell cycle progression, and inhibiting inflammatory reactions. Dual-luciferase activity demonstrated that RUNX2 was a direct target for miR-30a-5p and its expression was negatively and directly regulated by miR-30a-5p. Over-expression of RUNX2 weakened the inhibitory effect of miR-30a-5p on inflammatory injury. *In vivo*, over-expression of miR-30a-5p alleviated LPS-induced inflammatory responses and lung injury in LPS-administrated mice. Besides, miR-30a-5p repressed LPS-elevated phosphorylation levels of the signal transducer and activator of transcription 3 (STAT3) and c-Jun N-terminal kinase (JNK), IκBα degradation, and NF-κB p65 phosphorylation. In conclusion, miR-30a-5p ameliorates LPS-induced inflammatory injury in A549 cells and mice via targeting RUNX2 and related signaling pathways, thereby influencing the progression of ARDS.

Keywords

miR-30a-5p, RUNX2, LPS, ALI, ARDS

Date received: 26 August 2020; revised: 12 October 2020; accepted: 15 October 2020

Introduction

Acute lung injury/acute respiratory distress syndrome (ALI/ARDS) is caused by indirect or direct lung injury, and clinically characterized by disruption of the alveolar–capillary barrier and dysfunction of gas exchange.^{1,2} ALI/ARDS is histologically characterized by neutrophilic infiltration, lung edema, and exacerbated inflammatory response.^{3,4} Unfortunately, despite the current understanding of the pathophysiology and available treatment options, morbidity and mortality rates are still high due to infection diseases, especially the present outbreak of coronavirus disease 2019 (COVID-19). Therefore, it is essential to investigate the molecular mechanisms of ALI/ARDS.

MicroRNAs (miRNAs) are a class of conserved, 20–25-nucleotide and non-coding RNAs, which regulate gene expressions, cell differentiation, development, proliferation, and apoptosis.⁵ Previous studies have reported that aberrant expression of miRNAs was

associated with some inflammation-related diseases, suggesting the potential involvement of miRNAs in ARDS.⁶ To date, miR-30a-5p has been widely explored. For instance, miR-30a expression may contribute to protection from hyperoxic lung injury in female neonatal mice.⁷ MiR-30a shields cardiac myocytes against injury caused by ischemia/reperfusion.^{8,9} On the other hand, angiotensin II induces podocyte injury by activating the calcium/calceinurin pathway

¹Department of Pulmonary and Critical Care Medicine, The First Affiliated Hospital of Soochow University, Jiangsu, China

²Department of Intensive Care Unit, Shandong Provincial Third Hospital, Cheeloo College of Medicine, Shandong University, Shandong, China

Corresponding author:

Yanbin Chen, Department of Pulmonary and Critical Care Medicine, The First Affiliated Hospital of Soochow University, 899# Pinghai Road, Suzhou, Jiangsu 215000, China.
Email: chenyanbinsoochow@163.com



and reducing levels of miR-30 family members.¹⁰ However, the effect of miR-30a-5p on ARDS has not yet been well studied.

Here, cellular and murine models of inflammatory injury were constructed after exposure of LPS. Cell viability, apoptosis, cell cycle, and release of inflammatory cytokines were applied to evaluate inflammatory injury. Further, the functional role of miR-30a-5p and its possible target gene in LPS-induced cell injury was finally explored.

Materials and methods

Cell culture

Human lung epithelial cell line A549 and HEK-293T were purchased from BioVector NTCC Inc. (Beijing, China) and grown in RPMI-1640 medium containing 10% FBS (Gibco, Gran Island, NY, USA), penicillin/streptomycin (100 U/ml; Invitrogen; Carlsbad, CA, USA) at 5% CO₂ and 37°C. A549 cells were subjected to different concentration of LPS (0, 1, 5, 10, and 20 µg/ml) for different time points (12, 24, 48, and 72 h), and PBS was used as control.

Cell transfection

For the investigation of miR-30a-5p on biological behaviors of A549 cells, miR-30a-5p mimics and corresponding negative control (miR-NC) were synthesized by GenePharma (Shanghai, China). The transfection was carried out by using Lipofectamine 2000 (Invitrogen, Thermo Fisher Scientific, Inc.). The pcDNA3.1-RUNX2 was synthesized by Sangon Biotech (Shanghai) Co., Ltd., and transferred into cells using pcDNA3.1 (Invitrogen).

Murine lung injury model

First, our experiments conformed to the policies of Shandong Provincial Third Hospital Animal Ethical and Welfare Committee. In total, 40 female BALB/c mice (7–10-wk-old) were randomly assigned to four groups: PBS ($n=10$); LPS alone ($n=10$), agomir-30a-5p ($n=10$), and agomir-negative control (agomir-NC) ($n=10$). The ALI model was induced by a nasal drip with a lethal dose of LPS (10 mg/kg) in mice for 24 h. In control group, mice were initially injected intratracheally with 50 µl of PBS after 4 h. The agomir-30a-5p and agomir-NC were injected into the mice via tail vein for 72 h. The mice were anesthetized with 2% chloral hydrate (0.2 ml/10 g). Lungs were dissected (free of heart and trachea) and placed into Eppendorf tubes. Bronchoalveolar lavage fluid (BALF) was collected by flushing 1 ml ice-cold PBS back and forth three

times through a tracheal cannula and then centrifuged at 1000 *g* at 4°C.

RNA extraction and quantitative real-time PCR (qRT-PCR)

Total RNA including miRNA was isolated using TRIzol reagent (Invitrogen, Carlsbad, CA, USA). cDNA was synthesized using a High Capacity cDNA Reverse Transcription Kit (Applied Biosystems, Foster City, CA), and stored at –20°C. For quantification of miRNA, qRT-PCR was performed with an SYBR Green I Master Mix kit (Invitrogen) with the 7300 Real-Time PCR System (Applied Biosystems, USA). Finally, the expression was calculated by 2- $\Delta\Delta C_t$ method, and GAPDH or U6 was used to normalize the levels.

Western blotting

Cells were collected and lysed in the lysate (RIPA), where total protein was extracted for further determination of protein content in accordance with the BCA kit. According to results of the detection of protein concentration, 20 µl protein samples were extracted for Western blot assay. A 10% SDS-PAGE separation gel was then prepared. The sample was blocked for 2 h at room temperature with 5% skim milk powder buffer and then incubated with primary Abs overnight at 4°C. Then, the relative protein expression was determined after 1 h of secondary Ab incubation, electrochemiluminescence (ECL) development and photography.

Cell viability assay

CCK-8 reagent (Dojindo, Kumamoto, Japan) was employed to detect cell viability. First, cells (5×10^3 /ml per well) were seeded into 96-well plates, and then 10 µl/well of CCK-8 reagent was added to each well at 0, 24, 48, and 72 h, and incubated for 4 h at 37°C with 5% CO₂. After incubating, a microplate reader (Thermo Fisher Scientific) was used to read the values of OD 450 nm. Experiments were repeated in triplicate.

Apoptosis analysis

After 48 h of transfection, cells of each group were collected and washed in pre-cooled PBS. After that, 100 µl binding buffer was supplemented to re-suspend cells, followed by the addition and gentle mixing of 5 µl Annexin V-FITC and 5 µl propidium iodide (PI), in which cells were incubated for another 15 min before flow cytometry.

Cell cycle analysis

The cells were trypsinized and washed with PBS, then incubated with RNase A at 37°C for 30 min, and stained with 50 mg/ml PI at 4°C for 30 min. The distribution of cells in different phases of the cell cycle (G0/G1, S, and G2/M) was analyzed using a FACscan (Becton Dickinson, Franklin Lakes, NJ, USA).

ELISA

The levels of IL-1 β , IL-6, and TNF- α in the cell culture medium of different groups were detected using ELISA kits (BD Biosciences) according to the manufacturer's instructions. Optical density values were measured at 450 nm using an ELISA plate reader (Bio-Rad, Hercules, CA, USA).

Dual-luciferase reporter assay

HEK-293T cells were co-transfected with miR-30a-5p/miR-NC and pmirGLO-RUNX2-3'UTR-wild type (WT) and pmirGLO-RUNX2-3'UTR-mutation (MUT) (Promega, Madison, Wisconsin, USA). The cells were lysed 48 h after transfection. Then, luciferase activity was measured using a Dual-Luciferase Assay Kit (Promega) according to the manufacturer's instructions.

Statistical analysis

Results are expressed as the mean \pm SD of triplicate experiments. Statistical one-way ANOVA was performed using GraphPad Prism 5.0 software (GraphPad Software, Inc., Chicago, USA). $P < 0.05$ was considered statistically significant.

Results

LPS decreased miR-30a-5p expression, and induced cell apoptosis and inflammation

First, A549 cells were exposed to different concentration of LPS. We found that miR-30a-5p exhibited a significantly decreased level following the increase of LPS concentration (Figure 1a). MiR-30a-5p level was reduced for approximately 50% when A549 was subjected to 10 μ g/ml of LPS compared with PBS control group ($P < 0.01$) (Figure 1a), which can be applied for subsequent experiments. CCK-8 assay showed that cell viability obviously decreased in the presence of LPS ($P < 0.01$) (Figure 1b). Flow cytometry identified that the percentage of apoptotic cells was significantly increased after exposure of 10 μ g/ml of LPS ($P < 0.01$, Figure 1c). Likewise, cell cycle analysis revealed that LPS caused a dramatic accumulation in G1-phase and reduction in S-phase of A549 cells, whereas PBS

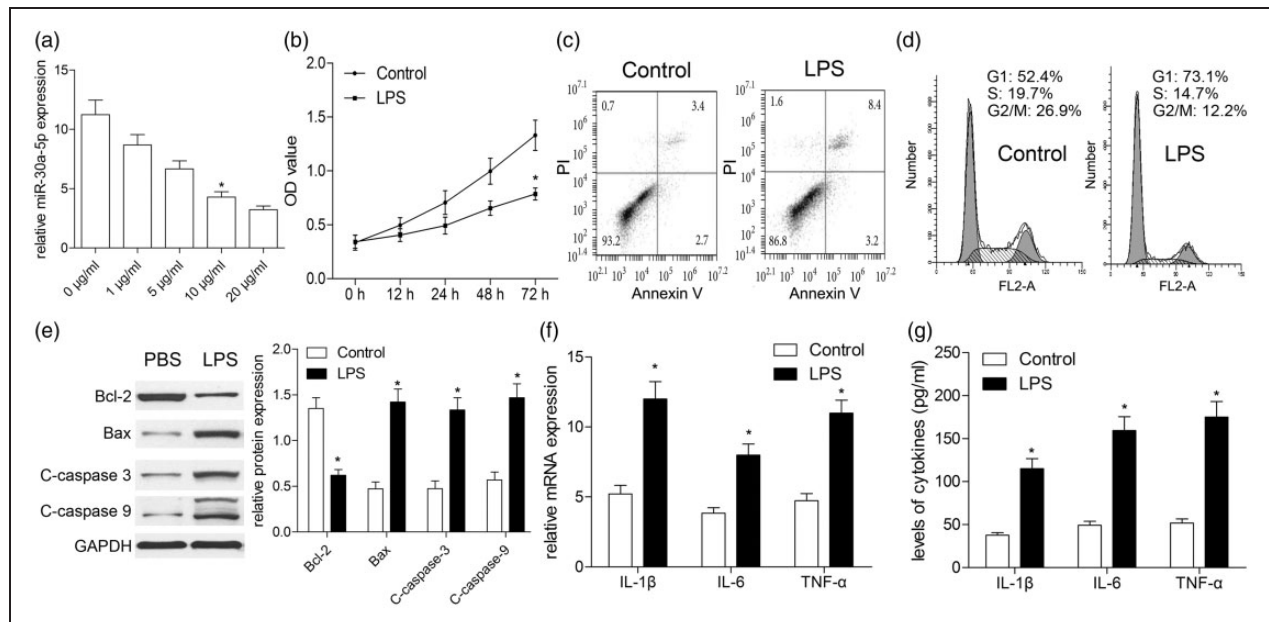


Figure 1. LPS exposure induces cell apoptosis and inflammation in A549 cells. A549 cells were subjected to different concentration of LPS. (a) Concentration curve of miR-30a-5p was plotted according to data of qRT-PCR. (b) Effect of LPS treatment with different concentration on cell viability. Cell apoptosis (c) and cell cycle analysis (d) were performed by flow cytometry. (e) Effect of LPS treatment on cell apoptosis-associated proteins (Bax, Bcl-2, and C-caspase-3/9) was determined by Western blotting. (f) Real-time PCR analyzed the mRNA expressions of inflammatory cytokines in LPS-induced A549 cells; (g) The secretion levels of IL-1 β , IL-6, and TNF- α were analyzed by ELISA. * $P < 0.01$, vs. PBS control, using repeated measures ANOVA test or Student's *t*-test.

control normally accelerated cell cycle progression of A549 cells to S-phase (Figure 1d). Further, Western blotting demonstrated that the apoptosis-related proteins, including Bax, cleaved-caspase-3 (C-caspase-3), and cleaved-caspase-9 (C-caspase-9), were markedly increased, while the Bcl-2 was significantly decreased (Figure 1e). Finally, results from qRT-PCR (Figure 1f) and ELISA (Figure 1g) showed that the expression levels of inflammatory cytokines (IL-1 β , IL-6, and TNF- α) obviously increased after incubation with LPS compared with the PBS control group ($P < 0.01$).

MiR-30a-5p alleviates LPS-induced cell apoptosis and inflammatory injury

miR-30a-5p mimics were transfected into A549 cells to augment the expression of miR-30a-5p. The transfection efficacy was measured by qRT-PCR, and the results showed a significantly increased expression of miR-30a-5p (Figure 2a). Then, miR-30a-5p over-expression significantly improved cell viability and decreased cell apoptosis which was induced by LPS ($P < 0.05$, Figure 2b, c), whereas miR-30a-5p did not change cell viability and apoptosis of A549 cells

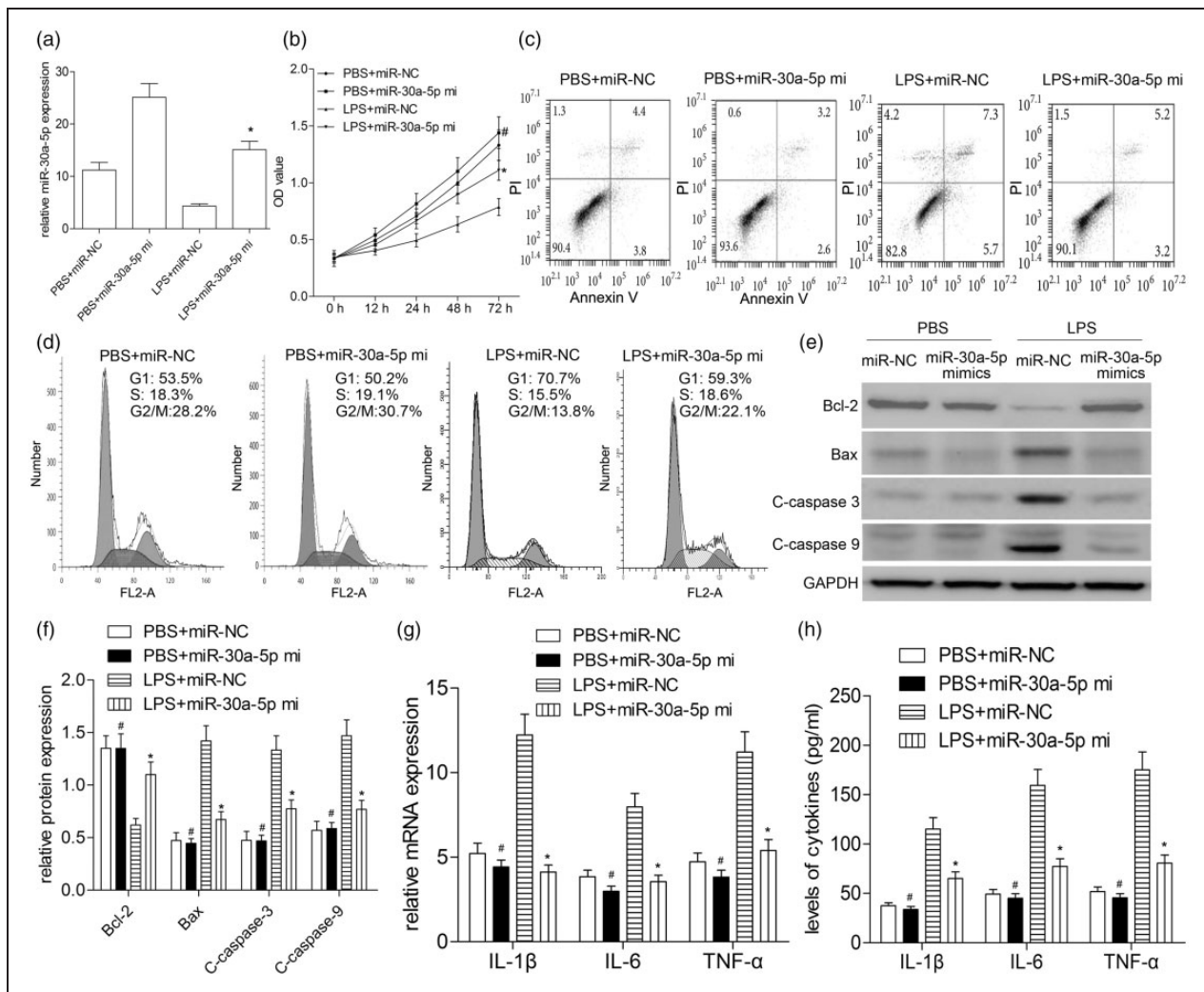


Figure 2. Over-expression of miR-30a-5p alleviates cell injury induced by LPS. (a) A549 cells were transfected with miR-30a-5p mimics; after transfection, the level of miR-30a-5p was determined by RT-qPCR. (b) Cell viability was determined by CCK-8 assay. (c) Cell apoptosis was analyzed by flow cytometry. (d) Cell cycle analysis was performed by flow cytometry. (e) The apoptosis-related protein expressions were determined by Western blotting, such as Bax, Bcl-2, C-caspase-3, and C-caspase-9. (f) Quantitative analysis was carried out according to the ratio between target protein and GAPDH levels from three different experiments with densitometry. (g) Real-time PCR analyzed the expressions of IL-1 β , IL-6, and TNF- α mRNAs in A549 cells treated with LPS. (h) The secretion levels of IL-1 β , IL-6 and TNF- α were analyzed by ELISA. # $P > 0.10$, vs. PBS + miR-NC; * $P < 0.01$, vs. LPS + miR-NC, using repeated measures ANOVA or Student's *t*-test

without LPS treatment ($P > 0.10$, Figure 2b, c). In the presence of LPS, flow cytometry analysis showed that miR-30a-5p dramatically increased the cell populations in S and G2/M phase and reduced the cell populations in G0/G1 phase (Figure 2d), indicating that miR-30a-5p reverses LPS-inhibited cell cycle progression. Besides, apoptosis-related proteins mentioned above were measured by Western blotting. Our findings revealed that the decreased expression of Bcl-2 and increased expressions of Bax, C-caspase-3, and C-caspase-9 by LPS were partially reversed by miR-30a-5p (Figure 2e, f). Subsequently, the impact of miR-30a-5p on the expressions of IL-1 β , IL-6, and TNF- α in LPS-treated A549 cells was further investigated using qRT-PCR and ELISA. As illustrated in Figure 2g and 2h, miR-30a-5p mimics effectively decreased the expressions of IL-1 β , IL-6, and TNF- α in A549 cells compared with miR-NC in the presence of LPS. When A549 cells were subjected to PBS treatment, miR-30a-5p mimics showed no significant differences from

miR-NC in cell cycle, apoptosis-related proteins, and production of inflammatory cytokines ($P > 0.10$). These findings indicated that miR-30a-5p protects against LPS-induced cell apoptosis and inflammatory injury.

MiR-30a-5p attenuates LPS-induced lung inflammation of mice

In our previous study, we had demonstrated that LPS successfully induced an ALI model of mice using pathological detection.¹¹ In the present study, we examined the expression of miR-30a-5p in the ALI mouse model. The RT-qPCR assay demonstrated that the levels of miR-30a-5p in the BALF, peripheral blood, and splenocytes as well as lung tissues were significantly reduced ($P < 0.01$, Figure 3a) in contrast to PBS control, suggesting that miR-30a-5p may be required for LPS-induced lung inflammation. For gain-of-function assay, the mice were administrated with agomiR-30a-5p or agomir-NC by tail intravenous injection at 24 h

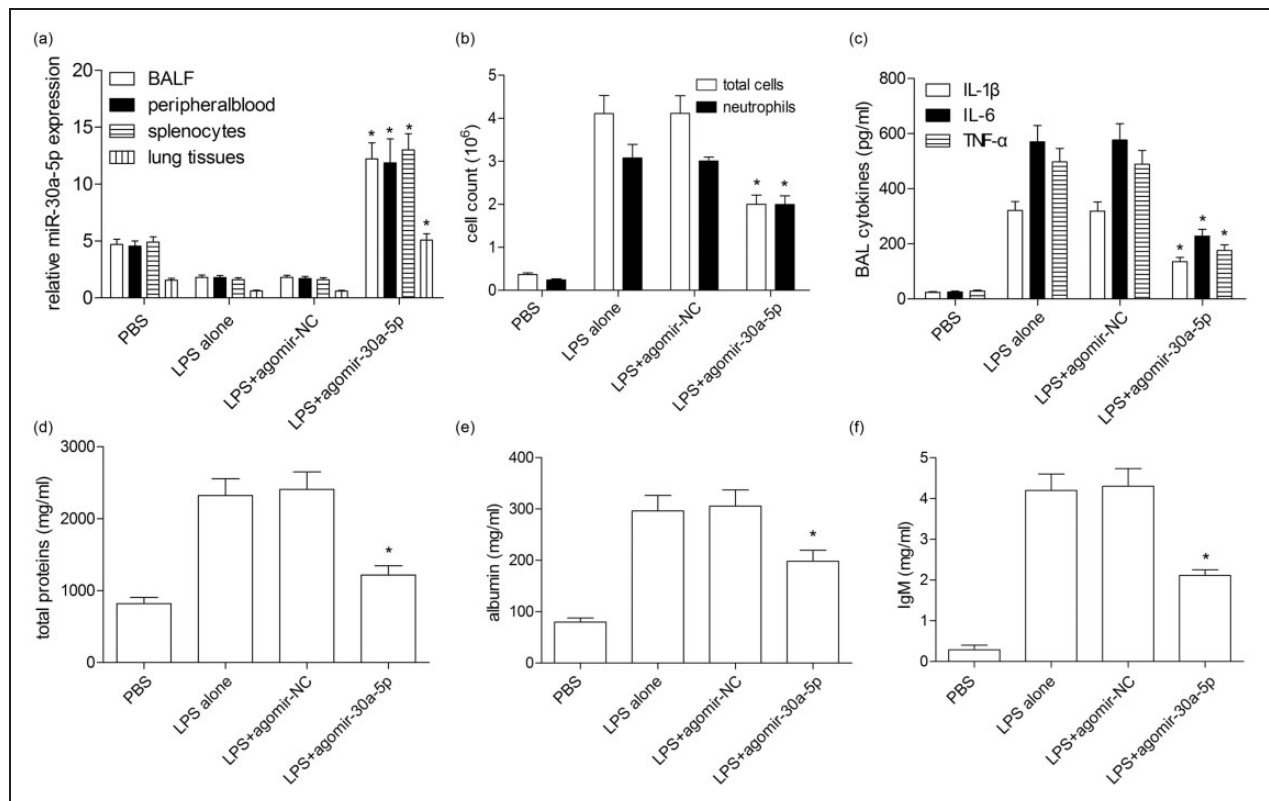


Figure 3. MiR-30a-5p ameliorates ALI/ARDS of LPS-induced mice. (a) The agomiR-30a-5p and agomir-NC were injected into the mice via tail vein before exposure to LPS. MiR-30a-5p expression in the BALF, peripheral blood, splenocytes, and lung tissues was detected by qRT-PCR. (b) Total leukocytes in the BALF were quantified by hemocytometric counting, and neutrophils were assessed based on their characteristic cell shapes. (c) The secretion levels of IL-1 β , IL-6, and TNF- α proteins were analyzed by ELISA. (d) Total protein levels in the BALF were assessed by Bradford assay. (e) Albumin levels (mg/ml) were measured by ELISA in the BALF. (f) Total IgM levels were measured by ELISA in the BALF. * $P < 0.01$, vs. PBS control or agomir-NC, using one-way ANOVA test with Tukey's post test.

prior to LPS stimulation. We found that miR-30a-5p mimics partially restored the level of miR-30a-5p in the BALF, peripheral blood, splenocytes, and lung tissues (Figure 3a). Then, miR-30a-5p impaired LPS-increased total white blood cell and neutrophils count (Figure 3b) as well as levels of inflammatory cytokines (Figure 3c) in the BALF. In addition, miR-30a-5p markedly reduced the elevated concentrations of total protein, albumin, and IgM in the BALF ($P < 0.01$, Figure 3d–f). These observations highlighted the involvement of miR-30a-5p in LPS-induced lung injury of mice.

RUNX2 is a direct target of miR-30a-5p

Using the TargetScan online prediction database, we found RUNX2 was a potential target gene of miR-30a-5p. The sequences of 3'-UTR of RUNX2 and miR-30a-5p are presented in Figure 4a. Then we found that miR-30a-5p over-expression remarkably inhibited RUNX2 protein expression in HEK-293T cells co-transfected with miR-30a-5p mimics and RUNX2 plasmids with WT 3'-UTR rather than MUT 3'-UTR ($P < 0.01$; Figure 4b). Subsequently, the dual-luciferase reporter assay showed that miR-30a-5p over-expression obviously reduced the luciferase activity of the reporters containing the WT 3'-UTR of RUNX2 compared with mimics control (Figure 4c), whereas no significant change in the luciferase activity was observed in those containing the MUT 3'-UTR of RUNX2 (Figure 4d). These results demonstrated the direct binding of miR-30a-5p with 3'-UTR of RUNX2.

RUNX2 weakens the inhibitory effect of miR-30a-5p on inflammatory injury

To confirm whether miR-30a-5p inhibited inflammatory response by regulating RUNX2 expression, we transfected the RUNX2 plasmids lacking its 3'-UTR into A549 cells with miR-30a-5p mimics. Western blotting results showed that endogenous RUNX2 protein was dramatically increased in A549 cells transfected with RUNX2 plasmids lacking 3'-UTR, as compared with those transfected with the vector control (Figure 5a). Moreover, miR-30a-5p-alleviated cell viability, -suppressed cell cycle, and -induced cell cycle progression was prevented when RUNX2 was up-regulated (Figure 5b–d). As expected, RUNX2 over-expression induced up-regulation of Bax, C-caspase-3, and C-caspase-9 ($P < 0.01$; Figure 5e), and secretion of inflammatory mRNAs ($P < 0.01$; Figure 5f) and cytokines ($P < 0.01$; Figure 5g). These results suggested RUNX2 is indeed involved in miR-30a-5p-mediated cell injury.

Effects of miR-30a-5p on LPS-induced activation of STAT3, JNK, and NF- κ B pathways

To assess the modulation of the signaling cascade related to LPS-induced ALI/ARDS, we determined the putative signal transduction pathways involved in the inflammatory reactions. Western blotting results revealed that LPS treatment (10 μ g/ml) significantly promoted STAT3 and JNK phosphorylation, and induced I κ B α degradation and NF- κ B p65 phosphorylation. On the other hand, miR-30a-5p obviously repressed STAT3 and JNK phosphorylation increased

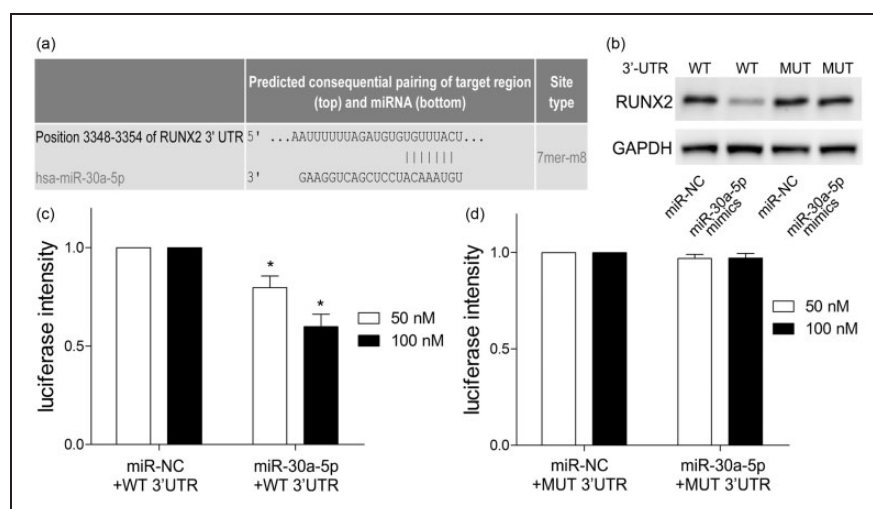


Figure 4. MiR-30a-5p directly targets RUNX2. (a) Schematic of the predicted miR-30a-5p binding sites in the 3'-UTR of RUNX2 mRNA was illustrated. (b) HEK-293T cells were co-transfected with miR-30a-5p mimics and pmirGLO-RUNX2 with WT or MUT 3'-UTR. RUNX2 protein expression was measured by Western blotting. Then luciferase reporter activity of WT (c) or MUT RUNX2 (d) in HEK-293T cells co-transfected with miR-30a-5p mimics or miR-NC was detected. * $P < 0.01$, vs. miR-NC, using two-way ANOVA.

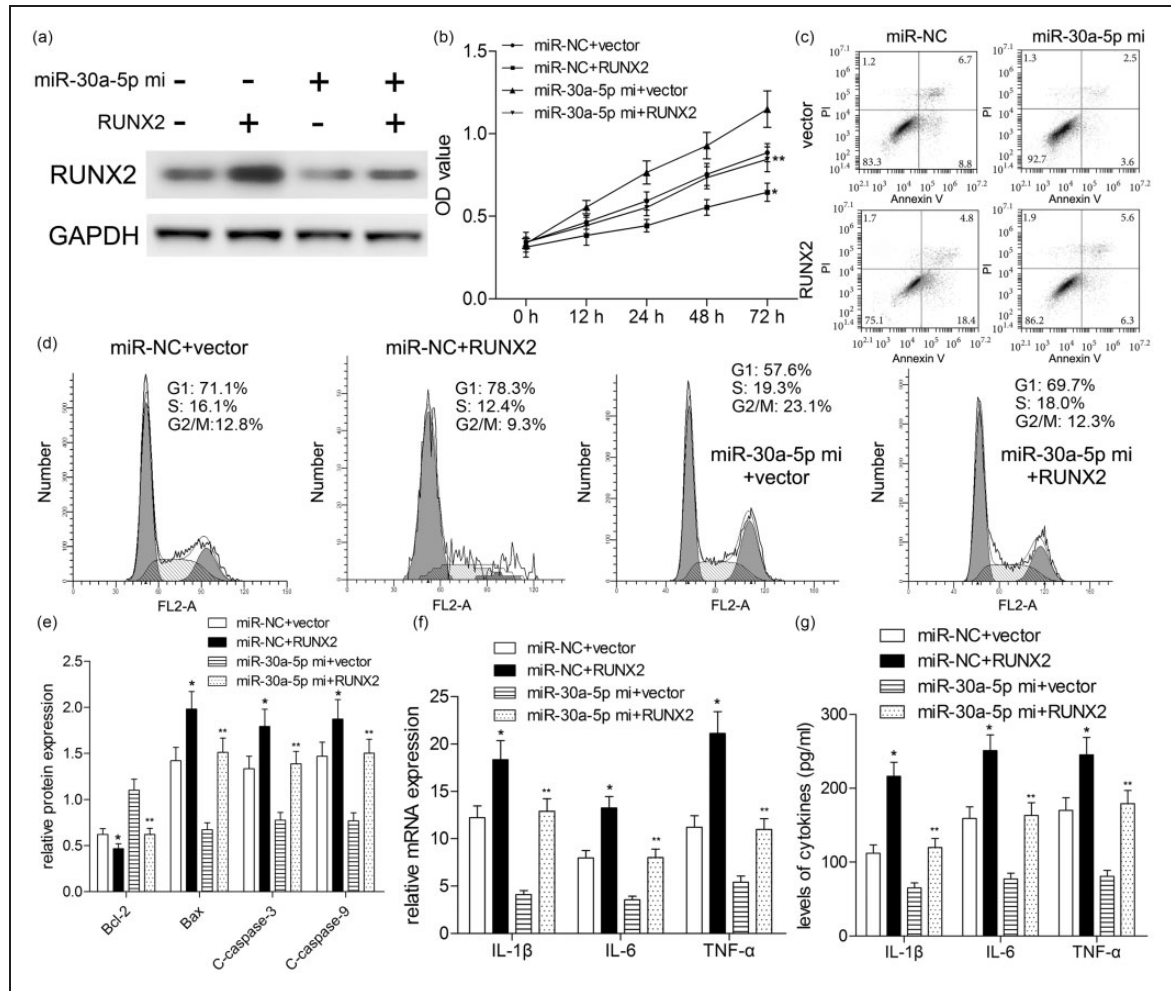


Figure 5. RUNX2 weakens the inhibitory effect of miR-30a-5p on inflammatory injury. Prior to LPS treatment (10 μ g/ml of LPS, 72 h), A549 cells were co-transfected with RUNX2 plasmids without WT 3'-UTR and miR-30a-5p mimics. (a) RUNX2 expression was determined by Western blotting. (b) Cell viability was subjected to CCK-8 assay. Effect of LPS treatment cell apoptosis (c) and cell cycle (d) analysis was investigated by flow cytometry. (e) Cell apoptosis-associated proteins were detected by Western blotting. (f) Real-time PCR analyzed the expressions of inflammatory cytokines. (g) Levels of inflammatory cytokines were measured by ELISA. * $P < 0.01$, vs. miR-NC + vector; ** $P < 0.01$, vs. miR-30a-5p+vector; using repeated measures ANOVA test or Student's *t*-test.

by LPS (Figure 6a), and significantly blocked the degradation of I κ B α by decreasing the phosphorylation level of I κ B α to reduce activation of NF- κ B characterized by decreased p65 phosphorylation level (Figure 6b, c). At the same time, in the absence of LPS, the above signaling pathway molecules in miR-30a-5p and miR-NC group were not markedly changed ($P > 0.10$, Figure 6). These results suggested that miR-30a-5p reduces the inflammatory response of A549 cells to LPS stimulation by inhibiting the phosphorylation levels of STAT3, JNK, p65, and I κ B α .

Discussion

Accumulating studies demonstrate that miRNAs exert essential roles in the initiation and progression of

various diseases.^{12,13} It is worth noting that numerous studies have identified that the level of miR-30a is decreased in varieties of tumor tissues. However, its role in ALI/ARDS was not well elucidated. In the present study, LPS-induced inflammatory injury of A549 cells and mice were used to simulate ALI/ARDS, and then the level and role of miR-30a-5p were investigated. *In vitro* assays revealed the expression of miR-30a-5p and A549 cell viability were effectively suppressed by LPS, whereas apoptosis and inflammatory cytokines were obviously increased, indicating that LPS induced inflammatory injury of A549 cells. *In vivo* assays showed that the level of miR-30a-5p in the BALF, peripheral blood, splenocytes, and lung tissues was significantly reduced by LPS treatment, suggesting that LPS induced inflammatory injury of lung tissue in mice.

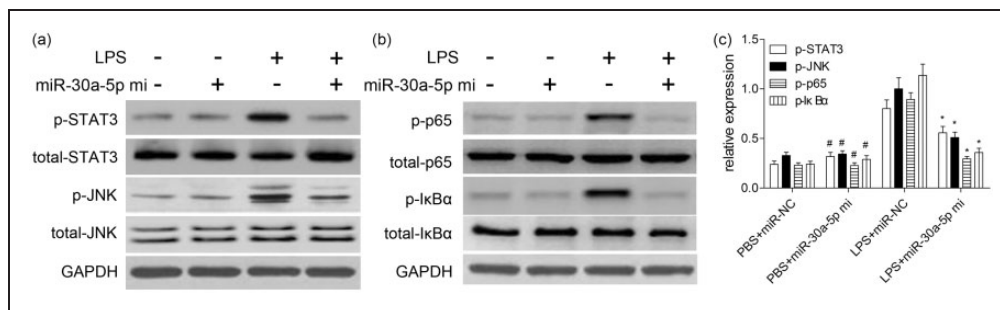


Figure 6. Effects of miR-30a-5p on LPS-induced activation of STAT3, JNK and NF- κ B pathways. Cells were plated at a density of 5×10^6 cells/dish in 60 mm culture dishes and treated with 10 μ g/ml LPS for 72 h. After preparation of the total protein, the phosphorylated and total forms of STAT3 (a), JNK (a), p65 (b) and I κ B α (b) were measured by Western blotting. (c) Quantitative analysis was carried out according to the ratio between target protein and GAPDH levels from three different experiments with densitometry. # $P > 0.10$, vs. PBS + miR-NC; * $P < 0.01$, vs. LPS + miR-NC; using repeated measures ANOVA test.

Further experiments may be applied to evaluate the effects of miR-30a-5p over-expression using transfection assay. We demonstrated that over-expression of miR-30a-5p improved cell viability and accelerated the cell cycle, and decreased apoptosis and the production of inflammatory cytokines, suggesting that miR-30a-5p could inhibit the inflammation injury. miRNAs are generally recognized as regulating gene expression post-transcriptionally by inhibiting translation or inducing target mRNA degradation.^{14,15} In this study, miR-30a-5p targeted the 3'-UTR of RUNX2 mRNA to reduce the expression of RUNX2 protein, which suggested that miR-30a-5p suppressed inflammatory injury by repressing translation of RUNX2 mRNA.

RUNX2 has been reported as a multifunctional transcription factor for osteoblast differentiation in previous studies, which exerts its effect on mesenchymal stem cell chondrogenic differentiation.¹⁶⁻¹⁹ As reported by recent studies, the expression of RUNX2 in Schwann cells and axons increased after sciatic nerve crush.¹⁶ RUNX2 over-expression accelerates progression of post-traumatic osteoarthritis in adult mice.¹⁷ miR-203 affects traumatic heterotopic ossification via reducing RUNX2 expression.¹⁸ CTRP13 attenuates vascular calcification through regulation of RUNX2 expression.¹⁹ Here, RUNX2 was a target gene of miR-30a-5p, and reversed miR-30a-5p-mediated inhibition effects, indicating that miR-30a-5p ameliorates LPS-induced inflammatory injury in human A549 cells via targeting RUNX2. Taking all results together, inhibition of RUNX2 combined with miR-30a-5p transfection may be a feasible therapeutic approach for ALI/ARDS.

NF- κ B transcription factors and the signaling pathways are central coordinators in innate and adaptive immune responses. STAT3 regulates the expression of a variety of genes in response to cellular stress, and thus

plays a key role in cell growth and apoptosis.²⁰ NF- κ B is activated during the inflammatory response to LPS, and is rapidly translocated into the nucleus after its detachment from I κ B α and binds to the target gene κ B locus to induce transcription of the target gene.²⁰ Apart from NF- κ B, the upstream signaling molecule JNK is activated by LPS and has been demonstrated to play a key role in NF- κ B activation.²¹ In the present study, we explored the signaling-based mechanisms of the anti-inflammatory effects of miR-30a-5p in A549 cells. Interestingly, we found that miR-30a-5p attenuated LPS-induced phosphorylation of STAT3 and JNK, and further affected the nuclear translocation of LPS-induced NF- κ B p65 in A549 cells.

In conclusion, this is the first study to demonstrate that miR-30a-5p regulated inflammatory reactions in LPS-induced ALI/ARDS via modulating RUNX2 expression and inflammatory signaling pathways, promoting new insights into the mechanisms and investigation of therapeutic strategies for patients with ALI/ARDS.

Compliance with ethical standards

All experimental animal procedures in this study conformed to the National Institutes of Health Guide for the Care and Use of Laboratory Animals and were approved by the Institutional Animal Care and Use Committee of Shandong Provincial Third Hospital.

Declaration of conflicting interests

The author(s) declared no potential conflicts of interest with respect to the research, authorship, and/or publication of this article.

Funding

The author(s) disclosed receipt of the following financial support for the research, authorship, and/or publication of this article: This work was supported by Medical and Health

Science and Technology Development Project of Shandong Province (2019WS453).

ORCID iD

Yanbin Chen  <https://orcid.org/0000-0001-8678-5934>

References

1. Ware LB, Koyama T, Billheimer DD, et al. Prognostic and pathogenetic value of combining clinical and biochemical indices in patients with acute lung injury. *Chest* 2010; 137(2): 288–296.
2. Badet M, Bayle F, Richard JC, et al. Comparison of optimal positive end-expiratory pressure and recruitment maneuvers during lung-protective mechanical ventilation in patients with acute lung injury/acute respiratory distress syndrome. *Respir Care* 2009; 54(7): 847–854.
3. Bellani G, Messa C, Guerra L, et al. Lungs of patients with acute respiratory distress syndrome show diffuse inflammation in normally aerated regions: A [18F]-fluoro-2-deoxy-D-glucose PET/CT study. *Crit Care Med* 2009; 37(7): 2216–2222.
4. Moradi M, Mojtahedzadeh M, Mandegari A, et al. The role of glutathione-S-transferase polymorphisms on clinical outcome of ALI/ARDS patient treated with N-acetylcysteine. *Respir Med* 2009; 103(3): 434–441.
5. Zhou T, Garcia JG and Zhang W. Integrating microRNAs into a system biology approach to acute lung injury. *Transl Res* 2011; 157(4): 180–190.
6. Olivieri F, Capri M, Bonafè M, et al. Circulating miRNAs and miRNA shuttles as biomarkers: Perspective trajectories of healthy and unhealthy aging. *Mech Ageing Dev* 2017; 165(Pt B): 162–170.
7. Zhang Y, Dong X and Lingappan K. Role of HIF-1 α -miR30a-Snail axis in neonatal hyperoxic lung injury. *Oxid Med Cell Longev* 2019; 2019: 8327486.
8. Li D, Wang J, Hou J, et al. Salvianolic acid B induced upregulation of miR-30a protects cardiac myocytes from ischemia/reperfusion injury. *BMC Complement Altern Med* 2016; 16: 336.
9. Guess MG, Barthel KK, Harrison BC, et al. miR-30 family microRNAs regulate myogenic differentiation and provide negative feedback on the microRNA pathway. *PLoS One* 2015; 10(2): e0118229.
10. Zhao Y, Wu J, Zhang M, et al. Angiotensin II induces calcium/calmodulin signaling and podocyte injury by downregulating microRNA-30 family members. *J Mol Med (Berl)* 2017; 95(8): 887–898.
11. Li P, Yao Y, Ma Y, et al. MiR-150 attenuates LPS-induced acute lung injury via targeting AKT3. *Int Immunopharmacol* 2019; 75: 105794.
12. Yuan S, Xiang Y, Wang G, et al. Hypoxia-sensitive LINC01436 is regulated by E2F6 and acts as an oncogene by targeting miR-30a-3p in non-small cell lung cancer. *Mol Oncol* 2019; 13(4): 840–856.
13. Jiang LH, Zhang HD and Tang JH. MiR-30a: A novel biomarker and potential therapeutic target for cancer. *J Oncol* 2018; 2018: 5167829.
14. Balatti V and Croce CM. MicroRNA dysregulation and multi-targeted therapy for cancer treatment. *Adv Biol Regul* 2019: 100669.
15. Torres JL, Novo-Veleiro I, Manzanedo L, et al. Role of microRNAs in alcohol-induced liver disorders and non-alcoholic fatty liver disease. *World J Gastroenterol* 2018; 24(36): 4104–4118.
16. Ding D, Zhang P, Liu Y, et al. Runx2 was correlated with neurite outgrowth and Schwann cell differentiation, migration after sciatic nerve crush. *Neurochem Res* 2018; 43(12): 2423–2434.
17. Catheline SE, Hoak D, Chang M, et al. Chondrocyte-specific RUNX2 overexpression accelerates post-traumatic osteoarthritis progression in adult mice. *J Bone Miner Res* 2019; 34(9): 1676–1689.
18. Tu B, Liu S, Yu B, et al. miR-203 inhibits the traumatic heterotopic ossification by targeting Runx2. *Cell Death Dis* 2016; 7(10): e2436.
19. Li Y, Wang W, Chao Y, et al. CTRP13 attenuates vascular calcification by regulating Runx2. *FASEB J* 2019; 33(8): 9627–9637.
20. Heo YJ, Choi SE, Jeon JY, et al. Visfatin induces inflammation and insulin resistance via the NF- κ B and STAT3 signaling pathways in hepatocytes. *J Diabetes Res* 2019; 2019: 4021623.
21. Kim HG, Shrestha B, Lim SY, et al. Cordycepin inhibits lipopolysaccharide-induced inflammation by the suppression of NF- κ B through Akt and p38 inhibition in RAW 264.7 macrophage cells. *Eur J Clin Pharmacol* 2006; 545: 192–199.